Cluster–Based Self–Assembly: Reversible Formation of Polyoxometalate Nanocones and Nanotubes

3 AUTHORS, INCLUDING:

Amjad Nisar
Tsinghua University
20 PUBLICATIONS **381** CITATIONS

Xun Wang
Tsinghua University
158 PUBLICATIONS **11,118** CITATIONS

CHEMISTRY OF MATERIALS
Article

Cluster-Based Self-Assembly: Reversible Formation of Polyoxometalate Nanocones and Nanotubes

Amjad Nisar, Jing Zhuang, and Xun Wang*

Department of Chemistry, Tsinghua University, Beijing 100084, P. R. China

Received May 13, 2009. Revised Manuscript Received July 15, 2009

Reversible self-assembly of Keggin structure polyoxometalate (POM) nanoclusters into nano-disks, nanocones, and nanotubes is described. The surface of POM clusters was modified by organic surfactant through single-phase approach. By carefully controlling and varying clusters surrounding environment, all assemblies were found to reverse into each other. The different assemblies and their evolutions from each other were studied by scanning electron microscopy and optical microscopy while the inner structure was investigated by transmission electron microscopy. The formation and transformation of different assembly shapes into each other is interpreted by considering electrostatic binding of surfactant molecules with the POM cluster, number of surfactant molecules attached, and particular surrounding environment arising from the optimized mixed solvent.

Introduction

Controlled self-assembling of nanobuilding blocks is an initial and key step toward development of advanced and functional superstructure and constitutes a highly important field of material science and engineering. In this context, atom/molecule and nanocrystal-based self-assembling dictated through both covalent and noncovalent interactions have been considered intensively in last few decades and a variety of nanoarchitectures and their potential applications in diverse fields such as medicines, catalysis, synthetic chemistry, sensing, etc. have been discovered. However, most of the assemblies restrict their applications to monofunctional and noncyclic systems, and the construction of reversible self-assembling structures has remained a mental and technical challenge.[1-4] Here, we present the cluster-based self-assemblies of large inorganic metal−oxygen clusters at room temperature which not only significant for their special nanocone and nanotube shapes but also for their totally reversible assembling behavior.

Among different areas of inorganic chemistry metal-oxide-based polyoxometalates (POM) molecular clusters represent a class of inorganic compounds that exhibit unmatched structural versatility and unique intrinsic properties.[5-9] Especially, the breakthrough in the modification of the POM surface by organic molecules extend the POMs access from aqueous media to the organic and biological materials, which provide another novel type of building blocks for the construction of nanoarchitectures.[10-13] In the last few years, a variety of work related to the self-assembling of POM-based hybrid clusters into different configurations has been reported but, in truth, it is limited to a few types of structures such as Langmuir−Blodgett films, honeycomb architectures, and single- and multilayer vesiclelike assemblies; therefore, there is a great need to focus on this area so that POM-based precisely designed multifunctional structures can be developed.[14-19] Among different morphologies, the conical and tubular structures are of high importance not only for their special shapes but also owing to the novel combination of access to three different chemical and physical regions of contact, inner−outer surfaces, and their ends. In this regard, a variety of materials and

*E-mail: wangxun@mail.tsinghua.edu.cn.
(1) Wang, X.; Li, Y. *Chem. Commun.* **2007,** 2901.
(2) Capito, R. M.; Azevedo, H. S.; Velichko, Y. S.; Mata, A.; Stupp, S. I. *Science* **2008,** *319,* 1812.
(3) Zhang, S. *Nat. Biotechnol.* **2003,** *21,* 1171.
(4) Shevchenko, E. V.; Talapin, D. V.; Kotov, N. A.; O'Brien, S.; Murray, C. B. *Nature* **2006,** *439,* 55.
(5) Kozhevnikov, I. V. *Chem. Rev.* **1998,** *98,* 171.
(6) Pope, M. T.; Müller, A. *Angew. Chem., Int. Ed.* **1991,** *30,* 34.
(7) Long, D.-L.; Burkholder, E.; Cronin, L. *Chem. Soc. Rev.* **2007,** *36,* 105.
(8) Coronado, E.; Giménez-Saiz, C.; Gómez-García, C. J. *Coord. Chem. Rev.* **2005,** *249,* 1776.
(9) Liu, T.; Diemann, E.; Li, H.; Dress, A. W. M.; Muller, A. *Nature* **2003,** *426,* 59.
(10) Kurth, D. G.; Lehmann, P.; Volkmer, D.; Colfen, H.; Koop, M. J.; Muller, A.; Du Chesne, A. *Chem.—Eur. J.* **2000,** *6,* 385.
(11) Proust, A.; Thouvenot, R.; Gouzerh, P. *Chem. Commun.* **2008,** 1837.
(12) Kurth, D. G.; Lehmann, P.; Volkmer, D.; Muller, A.; Schwahn, D. *J. Chem. Soc., Dalton Trans.* **2000,** 3989.
(13) Volkmer, D.; Bredenkotter, B.; Tellenbroker, J.; Kogerler, P.; Kurth, D. G.; Lehmann, P.; Schnablegger, H.; Schwahn, D.; Piepenbrink, M.; Krebs, B. *J. Am. Chem. Soc.* **2002,** *124,* 10489.
(14) Bu, W.; Li, H.; Sun, H.; Yin, S.; Wu, L. *J. Am. Chem. Soc.* **2005,** *127,* 8016.
(15) Clemente-León, M.; Coronado, E.; Gómez-García, C. J.; Mingotaud, C.; Ravaine, S.; Romualdo-Torres, G.; Delhaès, P. *Chem.—Eur. J.* **2005,** *11,* 3979.
(16) Fan, D.; Jia, X.; Tang, P.; Hao, J.; Liu, T. *Angew. Chem., Int. Ed.* **2007,** *46,* 3342.
(17) Zhang, J.; Song, Y.-F.; Cronin, L.; Liu, T. *J. Am. Chem. Soc.* **2008,** *130,* 14408.
(18) Nakanishi, T.; Michinobu, T.; Yoshida, K.; Shirahata, N.; Ariga, K.; Möwald, H.; Kurth, D. G. *Adv. Mater.* **2008,** *20,* 443.
(19) Sun, H.; Bu, W.; Li, Y.; Li, H.; Wu, L.; Sun, C.; Dong, B.; Dou, R.; Chi, L.; Schaefer, A. *Langmuir* **2008,** *24,* 4693.

their potential applications in different fields have been reported.[20−30] In this paper, we present the cluster-based self-assemblies of large inorganic metal−oxygen clusters to develop novel POM nanodisks, nanocones, and nanotubes at room temperature. Although, there are several reports about the self-assembling of different types of materials into disk, conical, and tubular assemblies, to the best of our knowledge, there is no such report in the field of POM-based large hybrid clusters. We expect our endeavor may provide a new idea in self-assembling and drive more opportunities in cluster-based research in different fields of science.

Experimental Section

Chemicals. Dimethyldioctadecylammonium bromide (DODA·Br) was purchased from ACROS organics. Phosphotungstic acid ($H_3PW_{12}O_{40}$) and phosphomolybdic acid ($H_3PMo_{12}O_{40}$) were purchased from Sinopharm Chemical Reagent Co. Ltd. (SCRC) while the remaining chemicals used during experimental work were from Beijing Chemical Reagent Industry. All chemicals were of analytical reagent grade and used as received without any further purification. A single-phase approach[31] was adopted to prepare the C1 and C2 hybrid clusters. In the particular synthesis of C1, a weighed amount of $H_3PW_{12}O_{40}$ was added into DODA·Br solution in chloroform so that the molar ratio between DODA and $H_3PW_{12}O_{40}$ was kept to 3:1, respectively. The whole content was subjected to ultrasonication until a clear solution was obtained, and finally, C1 was collected by evaporation of the chloroform. The product was putted to be dry at room temperature until a constant weight was obtained. Phosphomolybdic acid based hybrid cluster (C2) was also obtained in the same way. ^{1}HNMR spectroscopy, thermogravimetric analysis, Fourier transform infrared spectrometry, and elemental measurements were performed (Figure 1A and the Supporting Information). The POM clusters disk, cone, and tube assemblies were obtained from the mixed solvent system of chloroform and *n*-butanol at the optimized volume ratios. Instrumentation and sample preparation details are given in the Supporting Information.

Characterization. The size, morphology, and other structural details of the POM hybrid cluster disk, conical, and tubular assemblies were studied by JEOL JEM-1200EX and FEI Tecnai G2 F20 S-Twin transmission electron microscopes (TEM) while

TEM samples were prepared on carbon coated copper grid by a dip coating technique. Scanning electron microscopy (SEM) investigations were performed on FEI Sirion 200 scanning electron microscope by depositing the sample on a silicon wafer. Small angle X-ray diffraction patterns of the dried powdered samples of particular shapes were obtained by Rigaku D/max-2500/PC X-ray diffractometer using Cu Kα radiation (λ = 1.5418 Å). Thermogravimetric analyses were obtained by TA Instruments Q5000 IR thermogravimetric analyzer (TGA). Fourier transform infrared spectrometry (FTIR) was performed on Nicolet AVATAR 360 ESP FTIR. NMR spectra and elemental analysis were obtained by JEOL ECA-600 NMR spectrometer and elemental EAI CE-440 elemental analyzer, respectively.

Results and Discussion

POM Cluster-Based Nanodisks. A single phase approach[31] was adopted to prepare the POM Keggin ions, such as $[PW_{12}O_{40}]^{3−}$ and $[PMo_{12}O_{40}]^{3−}$, hybrid clusters. Owing to good stability and long alky chain dimethyldioctadecylammonium bromide (DODA·Br) was selected as organic surfactant which provides ease to study the self-assembling mechanism at different stages. The fundamental characterizations of the clusters, such as (DODA)$_3$-$PW_{12}O_{40}$ (C1) and $(DODA)_3PMo_{12}O_{40}$ (C2), were performed by ^{1}HNMR spectroscopy, thermogravimetric analysis, Fourier transform infrared spectrometry, and elemental measurements (Figure 1a and the Supporting Information). A mixed solvent system of chloroform and *n*-butanol was adopted and employed throughout the whole work. With optimization and careful control of chloroform/butanol volume ratios, POM cluster reversible self-assemblies of disk, cone, and tube shapes were achieved. We started our work with the POM hybrid cluster C1. At the optimized chloroform/butanol volume of 3:1, C1 self-assembly into disks was obtained. Transmission electron microscopy (TEM), scanning electron microscopy (SEM) and optical microscopy investigations demonstrate that the assemblies are quite stable and exist in both solvent and solvent free dried state (Supporting Information, Figure S3a, b, and e and Figure 3a). The assemblies have circular shape and small thickness, so that, beneath assemblies can also be seen clearly. Magnified TEM images of the folded or curved portions of the discs explain that the assemblies are composed of an ordered lamellar pattern (Supporting Information, Figure S3e and f). The small-angle X-ray diffraction measurements of a dried sample further verified the lamellar nature with layer spacing of about 2.88 nm (Figure 1b). The energy dispersive spectroscopy coupled with the SEM shows the existence of the tungsten and carbon all over the assemblies which confirm the contribution of inorganic and organic parts in the hybrid clusters (Supporting Information, Figure S4).

Self-Assembly, Growth, and Reversible Behavior of POM Cluster Nanocones. To further explore the self-assembling behavior of the POM hybrid cluster, the chloroform/butanol ratio was varied and C1 cone assemblies were achieve at an optimized volume ratio of 2:1,

(20) Fan, S.; Chapline, M. G.; Franklin, N. R.; Tombler, T. W.; Cassell, A. M.; Dai, H. *Science* **1999**, *283*, 512.
(21) Kim, P.; Lieber, C. M. *Science* **1999**, *286*, 2148.
(22) Wong, S. S.; Joselevich, E.; Woolley, A. T.; Cheung, C. L.; Lieber, C. M. *Nature* **1998**, *394*, 52.
(23) Tahir, M. N.; Natalio, F.; Therese, H. A.; Yella, A.; Metz, N.; Shah, M. R.; Mugnaioli, E.; Berger, R.; Theato, P.; Schröder, H.-C.; Müller, W. E. G.; Tremel, W. *Adv. Funct. Mater.* **2009**, *19*, 285.
(24) Shrestha, N. K.; Macak, J. M.; Schmidt-Stein, F.; Hahn, R.; Mierke, C. T.; Fabry, B.; Schmuki, P. *Angew. Chem., Int. Ed.* **2009**, *48*, 969.
(25) Kreizman, R.; Hong, S. Y.; Sloan, J.; Popovitz-Biro, R.; Albu-Yaron, A.; Tobias, G.; Ballesteros, B.; Davis, B. G.; Green, M. L. H.; Tenne, R. *Angew. Chem., Int. Ed.* **2009**, *48*, 1230.
(26) Mishra, B. K.; Thomas, B. N. *J. Am. Chem. Soc.* **2002**, *124*, 6866.
(27) Klein, K. L.; Melechko, A. V.; Fowlkes, J. D.; Rack, P. D.; Hensley, D. K.; Meyer, H. M.; Allard, L. F.; McKnight, T. E.; Simpson, M. L. *J. Phys. Chem. B* **2006**, *110*, 4766.
(28) Sun, X.; Qiu, X.; Li, L.; Li, G. *Inorg. Chem.* **2008**, *47*, 4146.
(29) Krumeich, F.; Muhr, H. J.; Niederberger, M.; Bieri, F.; Schnyder, B.; Nesper, R. *J. Am. Chem. Soc.* **1999**, *121*, 8324.
(30) Zygmunt, J.; Krumeich, F.; Nesper, R. *Adv. Mater.* **2003**, *15*, 1538.
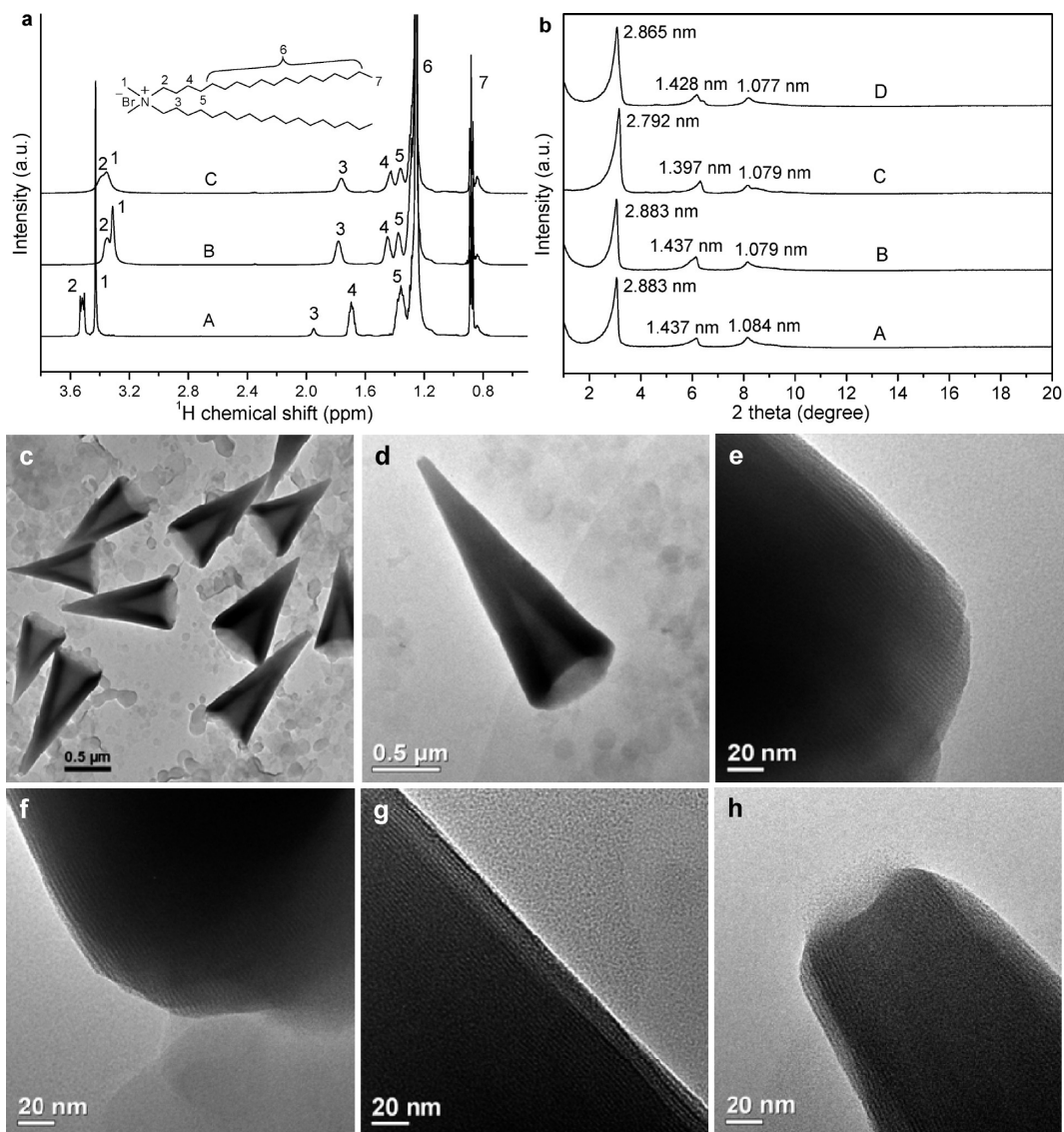(31) Nisar, A.; Xu, X.; Shen, S.; Hu, S.; Wang, X. *Adv. Funct. Mater.* **2009**, *19*, 860.

Figure 1. (a) ^{1}HNMR spectra of DODA·Br (A), (DODA)$_3$PW$_{12}$O$_{40}$ (B), and (DODA)$_3$PMo$_{12}$O$_{40}$ (C) in CDCl$_3$. (b) Small angle XRD patterns of (DODA)$_3$PW$_{12}$O$_{40}$ disk (A), cone (B), and tube (C) assemblies. Part D belongs to (DODA)$_3$PMo$_{12}$O$_{40}$ disk assemblies. (c) TEM image of a (DODA)$_3$PW$_{12}$O$_{40}$ bunch of cones at lower magnification. (d) One (DODA)$_3$PW$_{12}$O$_{40}$ cone at higher magnification. (e and f) Magnified image of the opening ends of the cone shown in part d. (g) Lamellar self-assembling pattern at the wall of the cone shown in part d. (h) Cone tip at higher magnification.

respectively. At this condition, disappearance of disk morphology and emergence of conical configuration was seen. The cones were found to consist of hollow interior with sloping curved walls and sharp tips (Figure 1c and d and Figure 2a−c). The TEM images of different parts of the cones, at higher magnification, demonstrate that the walls of cones are also composed of a lamellar pattern in which layers run straight from the open end to the tip or vice versa (Figure 1e−h). In contrast to the similar conical structure reported before, it was observed that the cones are not sealed at the tip but have a sharp opening (Figure 1h).[32] Careful observation of Figure 1h reveals that the clusters layers terminate at the tip without any twisting or linking with opposite side layers, which we think may be owed to flexible assembling behavior of the clusters which can rearrange to achieve maximum stability. It is worthwhile to note from SEM and optical

microscopy results that the formation of the cones does not occur through the simple rolling of the discs into conical shape, but it develops through the gradual molding of circular disk assemblies to produce a smooth conical shape (Figure 3b and the Supporting Information, Figure S6a−d). Previously, the similar conical shape evolution has been reported for graphite- and lipids-based cones.[33,34] The small-angle X-ray analysis of the dried cones showed no change in layer spacing; it was found to be same (2.88 nm) as in the disk assemblies (Figure 1b). In our experimentation, the disk and cone assemblies were found to be completely reversible between each other, and it was observed that one particular assembly can be generated again by reversing the solvent conditions. The reversible phenomenon of POM clusters can be attributed to the noncovalent electrostatic

(32) Zhang, G.; Jiang, X.; Wang, E. *Science* **2003**, *300*, 472.

(33) Krishnan, A.; Dujardin, E.; Treacy, M. M. J.; Hugdahl, J.; Lynum, S.; Ebbesen, T. W. *Nature* **1997**, *388*, 451.
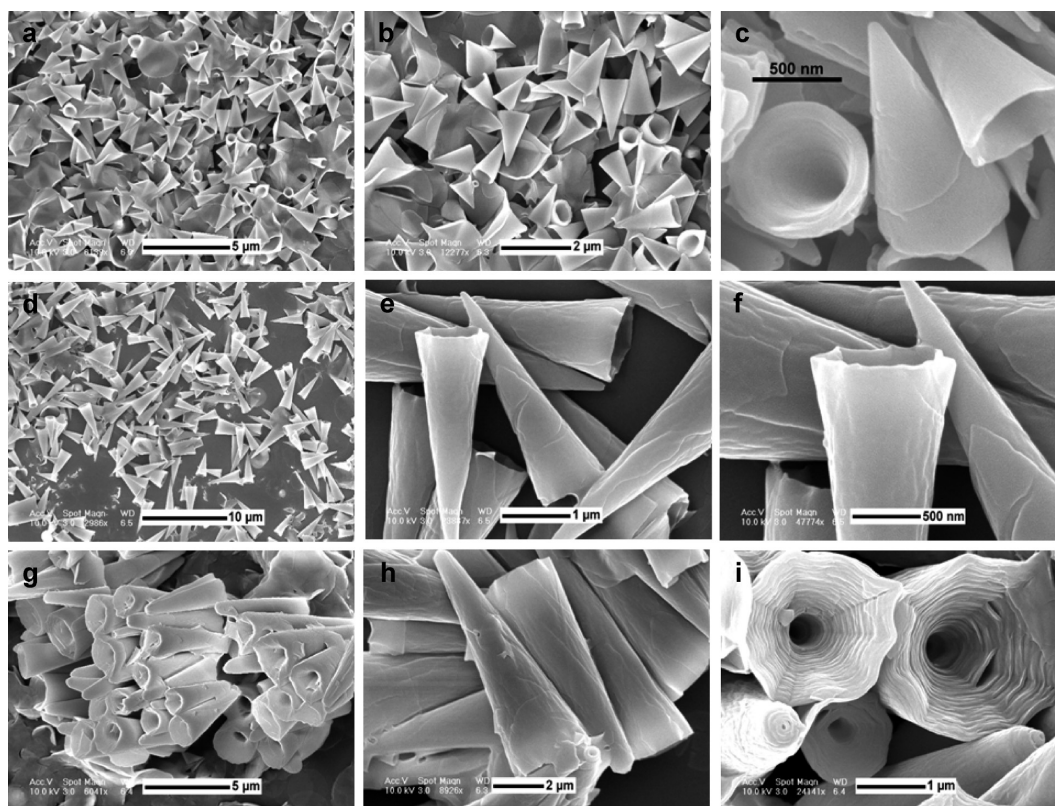(34) Douliez, J.-P. *J. Am. Chem. Soc.* **2005**, *127*, 15694.

Figure 2. SEM analysis of (DODA)$_3$PW$_{12}$O$_{40}$ cluster conical assemblies. (a–c) Cone images after 10 min of aging at lower and higher magnifications. (d–f) Cone images after 30 min of growth at different magnifications. (g and h) Cones after 1 and 2 h growth, respectively. (i) Magnified image of the cones' open ends and tips after 1 h of aging time.
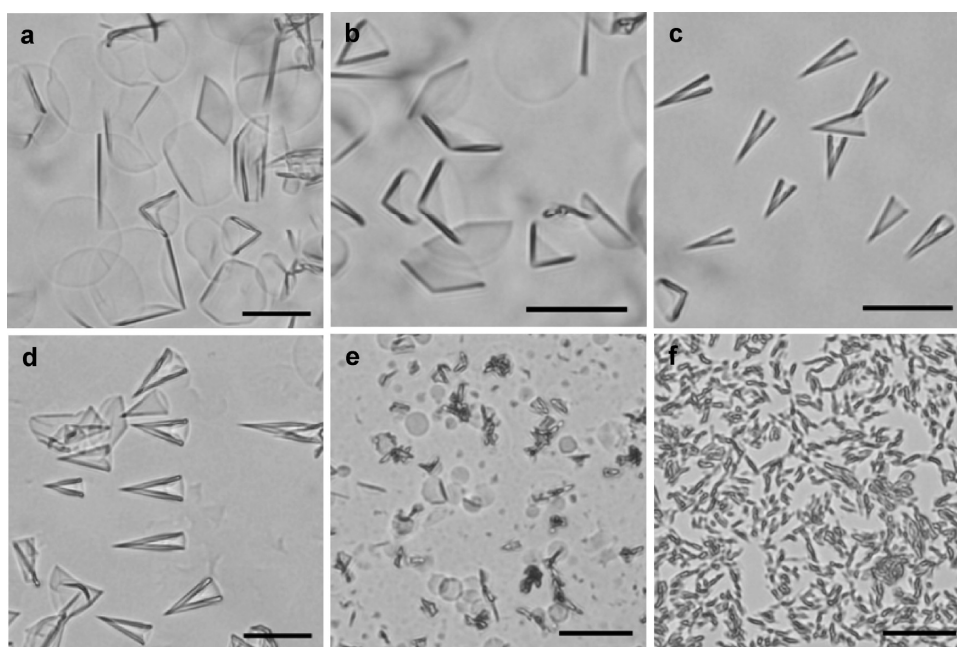

Figure 3. Optical microscopy study of (DODA)$_3$PW$_{12}$O$_{40}$ cluster assemblies. (a) Disk assemblies. (b) Cones of varying convex angle, showing transformation of disks into cones. (c) Cones after about 20 min of growth. (d) Cones after about 40 min of growth. (e) Disks after deformation of cones after about 12 h of aging. (f) Tubes after one day of aging. The scale bar in all images represents 5 μm.

interactions and amphiphilic nature of the POM hybrid clusters which provide the flexibility and dynamic capability to adopt new conditions quickly.

In order to fully pursue the POM hybrid clusters assembling behavior, the aging of the cones was performed both in the solvent and solvent free environment.

In the solvent free dried state, the conical shape was found to be quite stable, even for months, without any change in the size and lamellar nature, but in the solution environment, a very interesting process of cone growth was observed. The cone thickness and size were found to be tunable depending on the aging time in the solution

environment. Figure 2a–c shows the SEM images of cones after 10 min of self-assembling at different magnifications. The cone length lies in the range of $1.25–1.5\,\mu m$ with the outer diameter of about $0.6–0.8\,\mu m$ while the average wall thickness was measured to about 100 nm. The growth of the cone was observed in both axial and radial directions. The images in Figure 2d–f correspond to the cones which were obtained after 30 min of growth. The cones have grown to almost twice their initial dimensions both in length and outer diameter and lie in the range of about 3–4 and $1–1.25\,\mu m$, respectively. The growth may be due to the presence of unassembled monomers which with the passage of time come into contact with already built cones and adjust themselves into the conical shape according to the favored solvent conditions. After a further 1–2 h of aging, the length increases up to 5 and $10\,\mu m$ while the diameters are about 2 and $3\,\mu m$, respectively (Figure 2g and h). Close examination of the open ends and tips of the grown cones shows the presence of the circular loops at the open end as well as at the tip which reveals that the growth occurs in a layer by layer fashion and that the cone seems to be a roll of a continuous film (Figure 2i). Further, the presence of the sharp opening at the tip of the cones can also be seen, clearly, which supports the observations of TEM results. The comparable hollow interiors of the smaller and grown cones ($\sim0.5–0.6\,\mu m$) indicate cluster deposition at the outer surface and that cones primarily grow from the inner to the outer direction which may attributed to the easy access to the outer surface. The growth of cones with aging was also studied in the solution environment by optical microscopy which reveals similar results as those observed with SEM in a dried state (Figure 3c–d).

Evolution of Nanotubes from Nanocones and Their Reversible Behavior. On further aging of cones in the solvent environment for long times, a surprising phenomenon of disassembling of the conical structures and formation of tubes was observed. Figure 4a shows the TEM image of a collection of the tubular assemblies after 1 day of aging of cones in same optimized solvent environment as used in the case of cones. The high resolution TEM image of the specific region indicates the presence of the similar lamellar nature as in the case of disk and conical assemblies (Figure 4b). The tubular morphology was further verified both in the solvent and solvent free state by optical microscopy and SEM measurements, respectively (Figures 3f, 4c, and S5h). The magnified SEM images in Figure 4d and Figure S6i and j (Supporting Information) demonstrate that in contrast to the conical morphology the tubular structure formation originates from the rolling of the disk assemblies. Careful study of the transformation process revealed that after about 10 h of aging POM conical assemblies agglomerate with each other and start to collapse into a random filmlike morphology, and then after a further 2 h, they form the disk morphology, again, which later rolls to form tubes (Supporting Information Figure S6f–g and Figure 3e).

The small-angle X-ray diffraction of the dried tubes shows a layer spacing of about 2.79 nm with decrease of
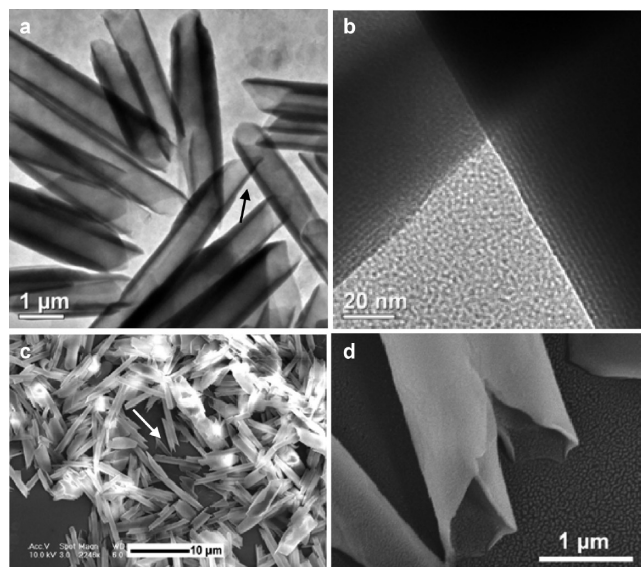

Figure 4. $(DODA)_3PW_{12}O_{40}$ cluster tubular assemblies. (a) TEM image of a collection of tubes after 1 d of aging time. (b) Magnified image of the marked region in part a. (c) SEM image of tubular assemblies. (d) Magnified image of marked region in part c.

about 0.1 nm compared to the initial disks and conical structures. The decrease in the layer spacing may be attributed to the increase in overall stiffness of the conical assemblies caused by the growth, and at a particular level of growth, the surfactant's alkyl chains get interlaced with each other to release this stiffness which ultimately results in the loss of the symmetry; finally, cones disassemble to form tubes. The reversible assembling phenomenon as observed for disk and cone structures was also investigated for tubular assemblies. It was found that tubular assemblies can be reversed back into disks and/or cones by increasing the amount of chloroform and reaffixing at a 3:1 and/or 2:1 chloroform/n-butanol volume ratio, respectively. The whole phenomenon of POM hybrid clusters self-assembly, which can be run in a reversible and cyclic way, can be described by the schematic illustration given in Figure 5a. As the cone and tube formations are reversible by tuning the solvent conditions, therefore this assembling behavior may possibly provide an opportunity to tune multifunctional catalysts in a variety of scientific and industrial applications.

Interpretation of POM Clusters Self-Assembling and Reversible Behavior. To understand the POM clusters self-assembling mechanism and reversible behavior between different shapes, the hybrid clusters' amphiphilic nature, the number of surfactant ions attached, and their possible rearrangement around the POM surface under particular solvent conditions were considered. According to POM chemistry, the Keggin structure consist of twelve MO_6 (M = Mo, W, etc.) octahedrons which by sharing their edges and corners create a shell around the central heteroatom (P, Si, etc.) tetrahedral (Figure 5b).[35,36] As the origin of negative charge (P, Si, etc.) lies in the center

(35) Keggin., J. F. *Proc. R. Soc. London Ser. A* **1934**, *144*, 75.
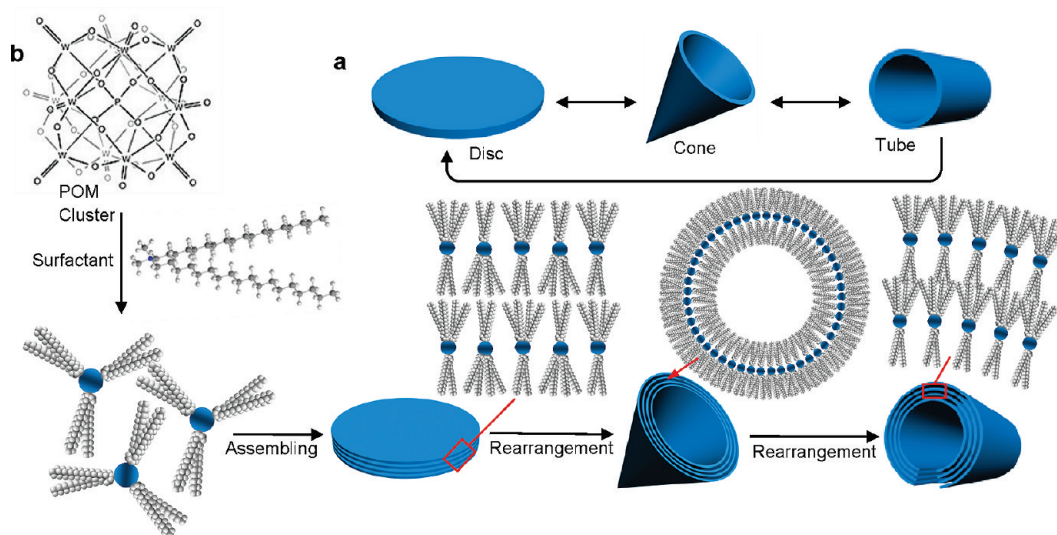(36) Day, V. W.; Klemperer, W. G. *Science* **1985**, *228*, 533.

Figure 5. Schematic illustration of POM clusters self-assembling. (a) Schematic illustration of POM cluster reversible self-assembling between nanodisks, nanocones, and nanotubes. (b) Schematic illustration of three-dimensional arrangement of POM clusters in different nanostructures.

of shell, the surfactant's positively charged ions bounded on the surface of Keggin ions by electrostatic interaction can be reasonably thought to be capable of rearrangement on the POM surface under the particular environmental conditions. The reported work about the rearrangement of surfactant cations on the POM surface subjected to the air/water interface supports our idea of surfactant ion rearrangement on the POM surface under particular environmental conditions.[37,38] As the $(DODA)_3PW_{12}O_{40}$ hybrid cluster has three surfactant ions, so it may be expected that, under particular surrounding forces when POM clusters come into contact with each other, the DODA ions rearrange on the POM surface so that one DODA ion orients to one side while the other two go toward opposite sides. In disk assemblies, which are obtained at relatively lower polarity conditions, it is expected that surfactant ions arrange themselves in alternative positions according to the adjacent hybrid clusters and result in a straight surface. While at relatively high polarity conditions, one surfactant ion comes toward inner direction while the other two go to outer directions and ultimately result in curved cone and tube assemblies (Figure 5b). Previously, published reports about hybrid POMs with four surfactant ions to form spherical vesicles[31,38] also support our assumption of the formation of disk, cone, and tube shapes due to a specific number (three) of surfactant ions being attached. Similarly, the reversible behavior of disk, cone, and tube assemblies may also be owed to the DODA ions' flexible rearrangement at the POM surface under a particular surrounding environment. Therefore, we believe, assembling of POM clusters into disk, conical, and tubular shapes strongly depends on the number of surfactant ions attached and their possible arrangement on the POM surface under certain surrounding forces.
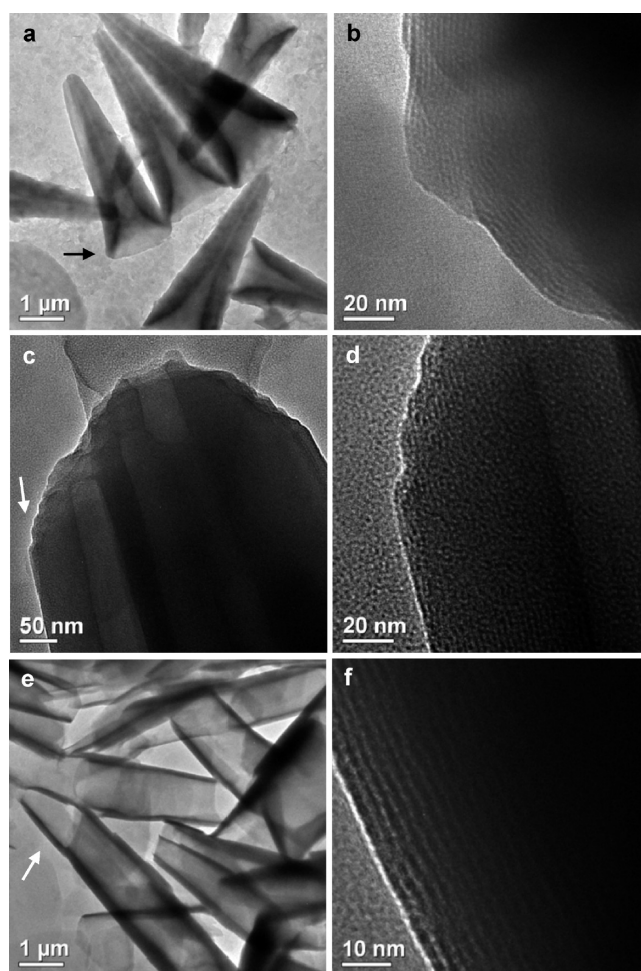

Figure 6. TEM images of $(DODA)_3PMo_{12}O_{40}$ cluster conical and tubular assemblies. (a) Bunch of cones at lower magnification. (b) Magnified image of the region marked by arrow in part a. (c) Tip of cone marked in part a. (d) Magnified image of marked part of the tip in part c. (e) Tubes after 1 d of aging in the reaction mixture. (f) Images of the region marked by the arrow in part e at higher magnification.

(37) Bu, W. F.; Fan, H. L.; Wu, L. X.; Hou, X. L.; Hu, C. W.; Zhang, G.; Zhang, X. *Langmuir* **2002**, *18*, 6398.
(38) Li, H.; Sun, H.; Qi, W.; Xu, M.; Wu, L. *Angew. Chem., Int. Ed.* **2007**, *46*, 1300.

To generalize and check the validity of our approach to alike POM clusters, we applied our technique to C2, in the

same solvent system. In the case of C2, similar phenomenon of self-assembling into disks, cones, and tubes was found (Supporting Information, Figure S3, and Figure 6). TEM results illustrate the existence of a similar layered pattern as in the case of C1 clusters. Small angle X-ray analysis of dried disk assemblies (Figure 1b) revealed the similar layer spacing of about 2.86 nm which may be owed to the fact that both W and Mo are d^0 valence and have equivalent ionic radii. Further, in C2 clusters, similar growth of cones was also seen with aging which is clear from the existence of spiral loops at the tip of cone (Figure 6c).

Conclusions

In summary, POM cluster-based multiple and dynamically reversible nanoarchitectures have been designed by carefully controlling surrounding environments and by choosing the appropriate solvent system. The driving forces behind the reversible formation of disk, cone, and tube shape assemblies lie in number of surfactant molecules attached and their specific arrangement around the POM in particular surrounding environments. The hollow interior of POM cones and tubes can act as a container for foreign materials to discover new combinatorial applications. Similarly, the mesoporous nature of assemblies can act as a host for metal nanocrystals which may play important roles in catalysis. We believe the reported POM nanoarchitectures can amplify the POMs capabilities in a variety of scientific fields, such as electrochemistry, materials science, catalysis, medicine, etc. and may prove to contribute to new and advanced functional materials.

Supporting Information Available: FTIR spectra of POM clusters (C1 and C2) and surfactant, elemental analysis, TGA analysis, energy dispersive spectroscopy (EDS) spectra, and SEM images of cones and tubes. This material is available free of charge via the Internet at http://pubs.acs.org.